5th US Combustion Meeting
Organized by the Western States Section of the Combustion Institute
and Hosted by the University of California at San Diego
March 25-28, 2007

NOx from Gaseous and Prevaporized Fuels Burned Lean-Premixed at Atmospheric Pressure in Single-Jet Stirred Reactors

Philip Malte, Ryan Edmonds[1], Andrew Campbell Lee[2], Igor Novosselov, Brian Polagye, and Keith Boyd Fackler

Energy and Environmental Combustion Laboratory
Department of Mechanical Engineering
University of Washington
Seattle, Washington 98195-2600

Current affiliations:
1. *Ramgen Power Systems, Bellevue, WA*
2. *Dept of Mech Engr, Stanford University, Stanford, CA*

NOx measured for lean-premixed combustion of several gaseous fuels (methane, ethylene, propane, blends of C_1-C_4 alkanes, hydrogen, and blends of H_2-CO) and prevaporized liquid fuels (light naphtha and #2 diesel) is reported. Many of the experiments are conducted for a combustion temperature of 1790K, measured for the recirculation zone of the jet-stirred reactor. Pressure is 1 atm and inlet temperature is 425 to 825K. Reactor mean residence time is 1.3-4.5 milliseconds, though some experiments on hydrogen are conducted at longer times. Two jet stirred reactor sizes are used: 16 and 64 cm^3. Both use a single jet to feed the fuel-air mixture into the reactor. Jet diameters are 4, 5.6, and 9 mm. Combustion is stabilized by stagnation of the jet at the closed end of the reactor and by the interaction of the reactants of the feed jet with the recirculating and exiting gases. Several fuel-air injectors are used: a staged prevaporizer-premixer for the liquid fuels, as well as for several of the gaseous fuels, and tube and spoke premixers that connect directly to the reactor. Laser Rayleigh scattering measurements have been used to examine the degree of vaporization and mixedness of the liquid fuel-air feed jets. The NOx for methane (1790K, 4 ms) is 4-5 ppmv (15% O_2 dry), and serves as a baseline. As the C/H ratio of the fuel increases, with temperature held constant, and residence time held approximately constant, NOx increases. These results have application to low (single-digit) NOx combustion in industrial equipment. Since lean-premixed NOx can be a weak function of pressure, the results have application to power generation and pipeline gas turbines. Initial experimental results on hydrogen flashback are also reported, showing conditions of fuel-air equivalence ratio and injector velocity that induce burning in the one of the tube and spoke injectors.

1. Introduction to Reactor Systems

The classic jet-stirred reactor of Longwell and Weiss [1] used a spherical center-body drilled with many small holes for feeding the fuel-air mixture into the reactor at high velocity. Through the use of the multiple jets of small diameter and high velocity, the

well-stirred reactor condition, with time-mean spatial uniformity in temperature and composition, could be attained. Subsequent reactor designs were based on a spherical sector, rather than the full spherical reactor.

Single-jet stirred reactors offer fluid mechanic simplicity, in that only a single jet and its surrounding field of entrained, recirculating gas must be considered. Pratt and Starkman [2] used a single-jet stirred reactor to explore ammonia-air combustion. Because of the relatively long chemical time of ammonia combustion, well-stirred reaction was feasible in the single-jet reactor. Pratt and Starkman based their design on the earlier single-jet reactor of Jenkins, Yumlu, and Spalding [3]. Subsequently, Malte and Pratt [4] used the single-jet reactor design to burn CO-air for the purpose of showing the significance of the N_2O mechanism in the formation of NO in continuous, high-intensity, lean-premixed combustion. The reactor of Malte and Pratt is shown in Figure 1. Combustion is stabilized by stagnation of the jet at the closed end of the reactor and by the interaction of the reactants of the feed jet with the recirculating and exiting gases. In addition to temperature and gas sampling along the paths shown in Figure 1, the probes can be angled for access to other parts of the reactor, and wall ports can be added for more access.

In the 1980s, Thornton and Malte [5] built and used a single-jet stirred reactor specialized for high-temperature oxidation studies (1000-1300K), rather than for combustion.

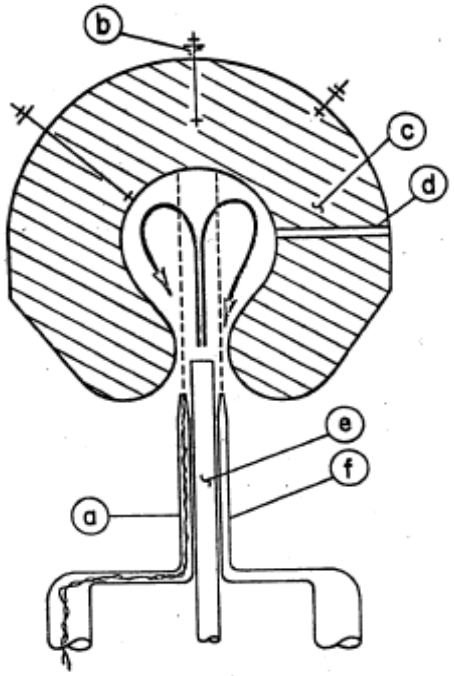

Figure 1: Single-jet stirred reactor of 67 cm^3 volume used by Malte and Pratt [4]. (a) traversing quartz enclosed thermocouple probe, (b) wall thermocouples, (c) ceramic reactor wall, (d) pressure tap, (e)reactant feed tube, and (f) traversing quartz sampling probe.

The fuel of interest was side-injected into the feed tube, which carried vitiated air from a lean H_2-air burner. The vitiated air with the fuel of interest added formed the jet of the reactor; this entered the reactor a short distance downstream of the side-injection point. Because only a small amount of fuel was added, yielding a small temperature increase above the vitiated air temperature, the chemical time was long and the reactor meet the well-stirred condition. Oxidation kinetics for CO, n-pentane, and hydrocarbons of interest in biomass combustion were examined.

Steele, Malte, and Kramlich [6] compared NOx formed in lean-premixed, jet-stirred reactors of both multi-jet and single-jet designs, and found little difference between NOx measured for the two designs when operated at the same temperate and residence time. Subsequently, single-jet stirred reactors have been used in our NOx research. Steele et al. [7] developed and used a high-pressure single-jet stirred reactor fired lean-premixed on methane to confirm the weak pressure dependence of NOx at elevated pressure. Rutar, Malte, and Kramlich [8] continued the work, showing a wide turn-down ratio, from a reactor residence time of 0.5 ms, where methane-fired reaction approached the well-stirred condition, to a residence time of 4 ms, for which the pressure drop of the premixer/reactor system was no more than 5%.

In this paper, we report experiments obtained in single-jet stirred reactors operated lean-premixed at atmospheric pressure where the focus is on NOx formation as a function of the fuel carbon to hydrogen ratio (based on fuel carbon to hydrogen atoms). The work builds on the original work of J.C.Y. Lee, Malte, and Benjamin [9], which included development of the staged prevaporizer-premixer (SPP) injector. Initial experiments on hydrogen flashback are also reported, showing conditions of fuel-air equivalence ratio (lean) and injector velocity that induce burning in a tube and spoke injector.

Figure 2 shows a drawing of the experimental system used by Edmonds [10]. Edmonds used a single-jet stirred reactor (JSR) of 16 cm^3 internal volume (nominal) mounted to the SPP. A nozzle (Inconel material, 4 mm diameter), is placed between the JSR and SPP and defines the jet entering the reactor. JSR width at the widest point is 25 mm; reactor height is 45 mm. Exhaust leaves the JSR through four drain holes surrounding the inlet jet of the reactor. Edmonds modified the SPP prior to use and performed maintenance, replacing seals and gaskets. Figure 3 shows a photograph of the JSR and SPP. Edmonds operated the system at higher air flow rates than J.C.Y. Lee et al. [9] (135-155 slpm versus 65 slpm). Consequently, the residence of the JSR was short: 1.3-1.5 ms. Three fuels were burned: methane, light naphtha, and low-sulfur #2 diesel.

A.C. Lee [11] continued work with the JSR-SPP system. The 16 cm^3 JSR (with 4 mm nozzle) was replaced with the 64 cm^3 JSR (with 5.6 mm nozzle), which has identical cavity geometry except for all dimensions being $4^{1/3}$ larger than the 16 cm^3 JSR. A.C. Lee increased the system air flow up to 205 slpm. JSR residence time increased to 3.2 to 4.3 ms, because of the 4-fold larger JSR volume. Propane and low-sulfur #2 diesel were the fuels burned. Laser Rayleigh scattering was used by A.C. Lee to examine the

outlet stream of the SPP for completeness of diesel fuel vaporization and goodness of mixing of the diesel fuel vapor in the air.

The 64 cm^3 JSR/SPP system was then used to study NOx as a function of C/H ratio for C_1-C_4 alkane blends burned lean-premixed at 1790K (nominal) and 3.6-3.8 ms. Unblended methane, propane, and ethylene were also burned, followed by H_2/CO/CO_2 blends and unblended H_2.

Following these experiments, the Inconel nozzle was replaced with a tube and spoke injector. This is shown in the drawing of Figure 4 underneath the JSR. The tube and spoke injector is placed between the JSR and the SPP.

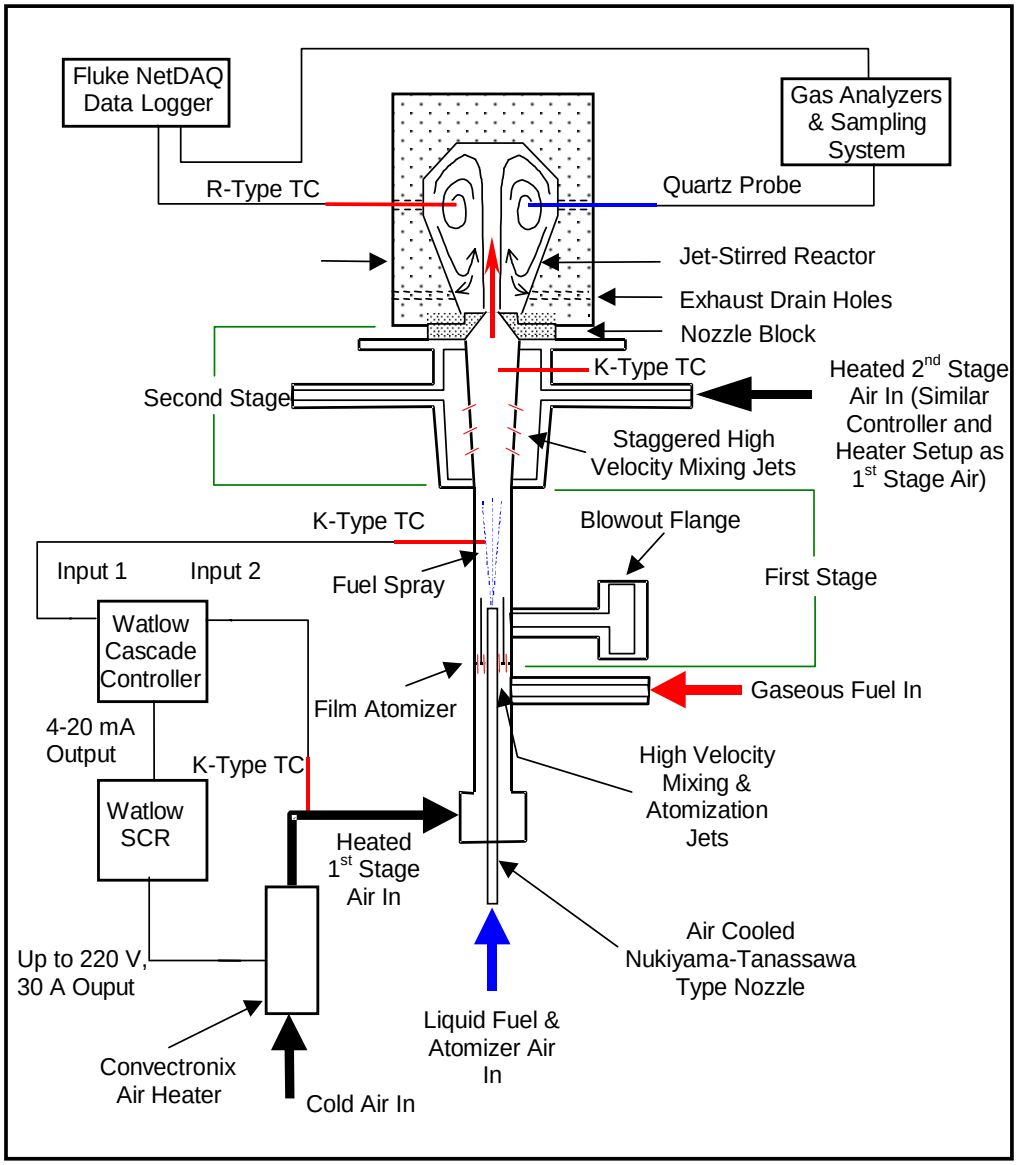

Figure 2: Single-jet stirred reactor with staged prevaporizer-premixer (SPP) injector. Edmonds [10] used a 16 cm^3 jet-stirred reactor with system operated at moderate flow rates; A.C. Lee [11] used a 64 cm^3 jet-stirred reactor with system operated at high flow rates.

Figure 3: Photograph of 16 cm^3 jet-stirred reactor and SPP used by Edmonds [10]. SPP modified by Edmonds from original by J.C.Y. Lee [9].

The SPP now serves only as the air preheater. Gaseous fuel enters through the spoke near the bottom of injector tube. The spoke (horizontal tube) has three small downstream pointing holes through which the fuel mixes with the air. The injector is stainless steel, except for the upper plate that interfaces to the JSR, which machined from Hastalloy. Six type K thermocouples (1/16 inch diameter) are placed just into the flow along the length of the injector tube. A seventh thermocouple (type R) is placed just into the flow at the Hastalloy plate. Two tube and spoke injectors have been built and used: 6.35 mm ID, and 9.0 mm ID. The 6.35 mm ID injector has been used in studies of hydrogen flashback. The 9.0 mm injector is used in studies which simulate the premixer-injector velocity of industrial gas turbines.

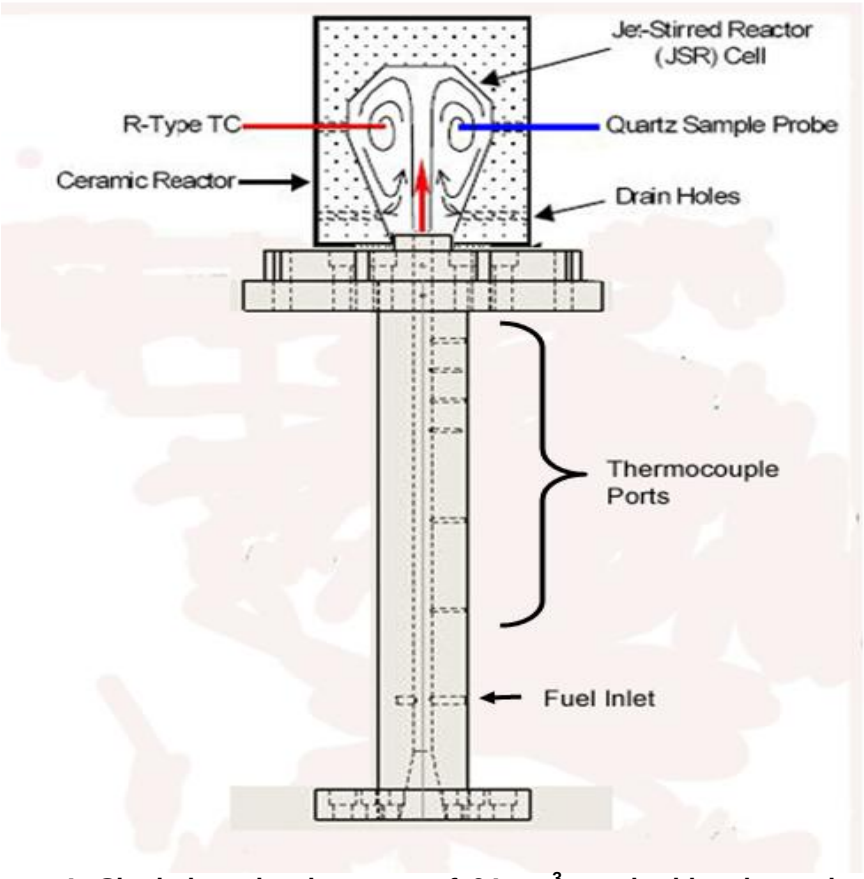

Figure 4: Single-jet stirred reactor of 64 cm^3 used with tube and spoke premixer-injector. Tube internal diameters of 6.35 and 9.0 mm used.

1. Experimental Results for NOx

The NOx measurements of Edmonds [10] and A.C. Lee [11] are plotted in Figure 5. The accompanying datasets are given in Tables A1, A2, and A3 of the Appendix. The conditions used by Edmonds and A.C. Lee are summarized in Table 1.

Table 1: SPP and JSR conditions used by Edmonds and A.C. Lee

	Edmonds [10]	A.C. Lee [11]
SPP		
Stage 1 temperature deg C	150-420	335-400
Stage 2 temperature deg C	250-550	500-525
Total air flow slpm	135-155	155-205
Total residence time ms	12.5-24	6-8.5
JSR		
Volume cm^3 / jet mm	16 / 4	64 / 5.6
Fuel-air equivalence ratio	0.47-0.65	0.53-0.54
Combustion temperature K	1790	1790
Residence time ms	1.3-1.5	3.2-4.3

The fuels studied by Edmonds are: methane, light naphtha ($C_{5.9}H_{12.5}$), and #2 diesel ($C_{13.8}H_{26.3}$). These are plotted from left to right on the lower curve in Figure 5. The contribution of the fuel-bound nitrogen to the NOx of the #2 diesel is estimated to be 1 ppmv (15% O_2 dry). A.C. Lee studied propane and the #2 diesel: these are plotted on the upper curve of Figure 5 as the middle and right points. The point at the left is 80% CH_4/20% C_3H_8 burned in the 64 cm^3 JSR with 9 mm tube and spoke injector, due to Fackler [12]. These data are listed in Table A3 of the Appendix. With the large jet, the inlet velocity is reduced to 67 m/s, versus 240-420 m/s for the other cases in Figure 5.

The reported measured combustion temperature has been corrected for heat loss from the thermocouple probe. Since the measurement is done within a nearly closed cavity with hot walls, the heat loss is small, of 30-40 degrees C. The thermocouple is of type R with an alumina coating to prevent surface catalysis. The thermocouple is inserted into the JSR at 2/3rd height (see Figure 2), and can be moved to profile the reactor. Generally, the temperature is found to be uniform within ±10 degrees C except for fall off in the jet zone of hydrocarbon fueled cases. For all measurements reported in this paper, the thermocouple is placed in the recirculation zone in the region of peak temperature. Temperature profiles are shown in [9] and [10].

Gas sampling is conducted using a small quartz probe inserted into the JSR at 2/3rd reactor height – though through a different port than the thermocouple. The sample probe is warm-water cooled, except for the uncooled probe tip that enters the reactor. The sampled gas is maintained warm in the sample line until the water of combustion is removed by impingers surrounded by an ice water bath. The dried sample gas is then drawn into an analyzer cart by a metal bellows pump and distributed into four gas analyzers placed in parallel: O_2 analyzer, non-dispersive infrared (NDIR) CO_2 analyzer, NDIR CO analyzer, and chemiluminescent NO-NOx analyzer. The analyzers are calibrated with standard gases. The standard sampling location is in the region of minimum CO in the recirculation zone of the JSR. Gaseous fuels and air are metered though mass flow controllers and liquid fuels are metered through rotometers.

Figure 6 shows CO profiles across two reactors: the 16 cm^3 JSR with 4 mm nozzle [10] and the 64 cm^3 JSR with 9 mm injector tube [12]. The radial location of the probe has been normalized by the radius of the reactor. The results from left to right indicate the flame structure of the JSR.

- Jet of reactants in the center of reactor.
- Flame zone encircling the jet, indicated by the peak CO.
- Recirculation zone, which forms the bulk of the reactor and allows the CO to burn out. However, since the pressure is low (1 atm) and residence time is short (<5 ms), the CO is unable to reach local equilibrium value. CO emission from the JSRs is in the 0.1-0.2 mole % range for the hydrocarbon cases.

NOx profiles are uniform for the bulk of the JSR, falling off only in the jet ([9] and [10]).

The premixing of fuel and air was examined by A.C. Lee [11], where laser Rayleigh scattering was used to examine the outlet stream of the SPP operated on #2 diesel fuel.

The measurements indicated no droplets exiting the SPP and the diesel vapor-air mixture was well mixed – this was inferred by noting that the standard deviation in the scattered light signal (collected at 90 degrees to the laser beam) was no more than about 10% of the mean scattered light signal. Thus, for the purposes of the present paper, it is assumed that the stream exiting the SPP and entering the JSR is fully vaporized (when liquid fuels are used) and well premixed.

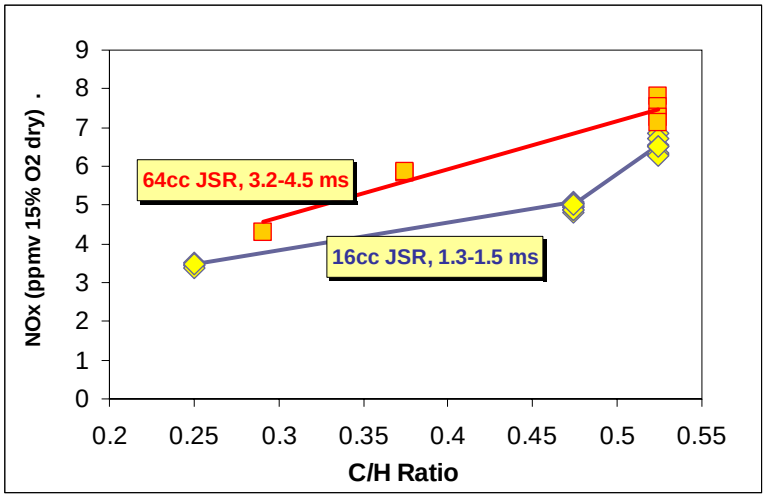

Figure 5: Measured NOx as a function of fuel carbon-to hydrogen ratio (by atom). 16 cm^3 JSR data are due to Edmonds [10]; 4 mm nozzle used; from left to right, the fuels are methane, light naphtha, and low-sulfur #2 diesel. 64 cm^3 JSR data are due to Fackler [12] and A.C. Lee [11]; Fackler used 9 mm nozzle, A.C. Lee used 5.6 mm nozzle; from left to right, the fuels are 80% methane/20% propane, propane, and low-sulfur #2 diesel. The combustion temperature is 1790K (nominal) in all cases.

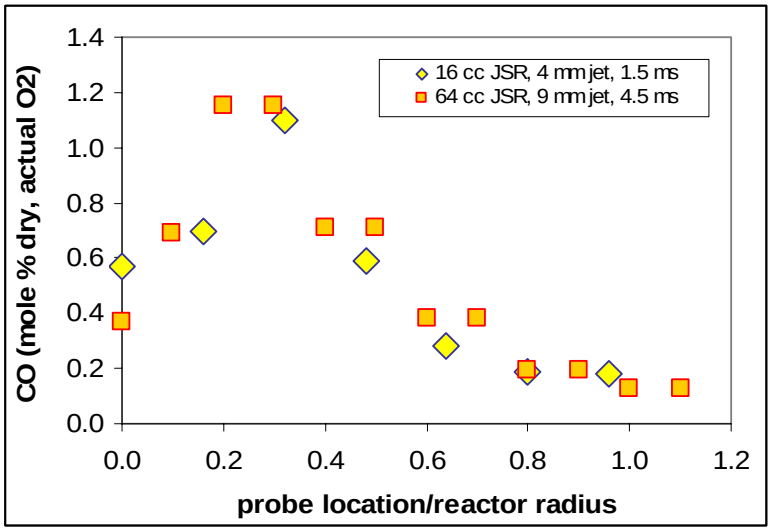

Figure 6: Measured CO profile across reactor, from centerline (at left) to reactor wall (1.0, at right). 16 cm^3 JSR operated on CH_4, 64 cm^3 JSR operated on 80% CH_4/20% C_3H_8.

Figure 7 shows NOx for gaseous hydrocarbons burned in the 64 cm^3 JSR with 5.6 mm nozzle. Combustion temperature is 1790 K (nominal) and the JSR residence time is 3.6-3.8 ms. The fuel at the left is methane, that at the right is ethylene, and that in the middle with a C/H ratio of 0.375 is propane. All other fuels are blends of C_1-C_4 alkanes. The dataset is given in Table A4 of the Appendix.

The trends seen from Figures 5, 6, and 7 for combustion of hydrocarbon fuels in the single-jet reactors are as follows:

- Increasing NOx with increasing C/H ratio (Figures 5 and 7). The results in this paper are similar to the original work of J.C.Y. Lee, Malte, and Benjamin [9].
- Increasing NOx with increasing JSR residence time (Figure 5).
- An error band of about 1 ppmv in the NOx measurement (Figures 5 and 7).
- Similar flame structure indicated in single-jet reactors of different volume and jet diameter (Figure 6).

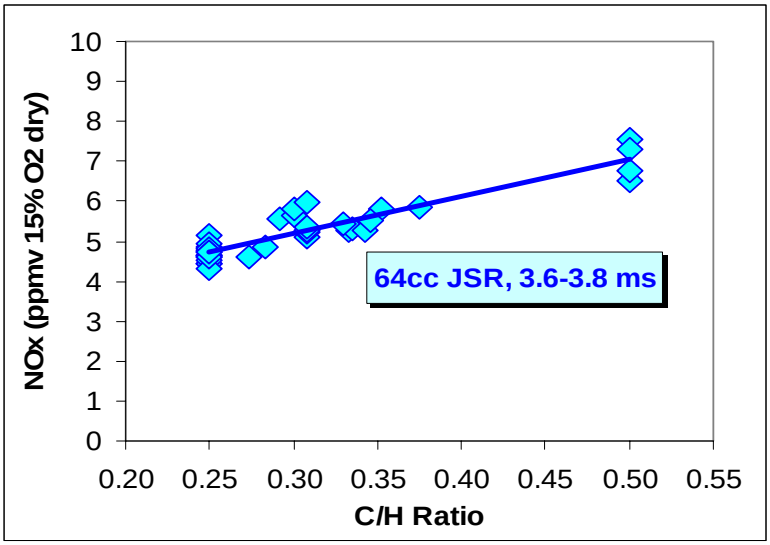

Figure 7: Measured NOx as a function of fuel carbon to hydrogen ratio (by atom) for methane (C/H = 0.25), ethylene (C/H = 0.5), and blends of C_1-C_4 alkanes. 64 cm^3 JSR with 5.6 mm nozzle. Combustion temperature is 1790K (nominal) in all cases. SPP injector outlet temperature = 150-300 C.

NOx is shown for the combustion of H_2/CO/CO_2 blends and unblended H_2 in Figures 8 and 9, respectively. The datasets are found in Tables A5 and A6 of the Appendix. The 64 cm^3 JSR with 5.6 mm nozzle was used. The practice of placing the thermocouple in the recirculation zone and setting the fuel flow for 1790 K corrected temperature was used. However, subsequently, upon temperature profiling of the JSR, peak temperature was found either in the jet or on the edge of the jet rather than in the recirculation zone. This is indicative of faster ignition of these fuels compared to the hydrocarbon fuels run. Thus, the picture of the structure of the reactor presented above requires modification for the H_2/CO/CO_2 and H_2 fuels, and the temperatures reported are likely 10 to 20 degrees C lower than the peak temperature.

The measurements of Figures 8 and 9 show the following trends:

- Less NOx formed from the $H_2/CO/CO_2$ fuels.
- Sensitivity (albeit weak) to SPP outlet temperature (JSR inlet temperature), which is not seen with the hydrocarbon fuels.
- NOx < 1 ppmv for hydrogen combustion for temperature < 1500 K (residence time about 4.6 ms). JSR did reach blow out condition in these experiments.

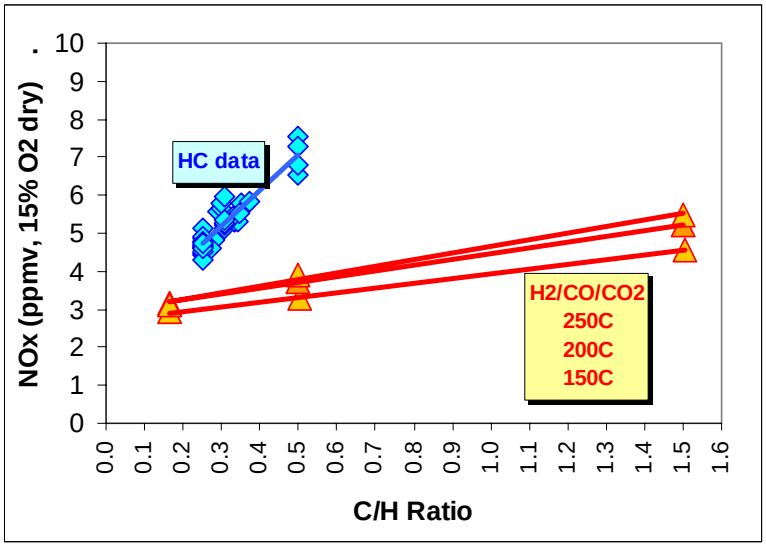

Figure 8: Measured NOx as a function of fuel carbon to hydrogen ratio (by atom) for $H_2/CO/CO_2$ blends. The CO_2 is 20 mole %; the C/H ratio is based on the CO/H_2 ratio. 64 cm^3 JSR with 5.6 mm nozzle. Combustion temperature is 1790K (nominal) in all cases. SPP injector outlet temperature = 150, 200, and 250 C. Hydrocarbon data from Figure 7 also shown.

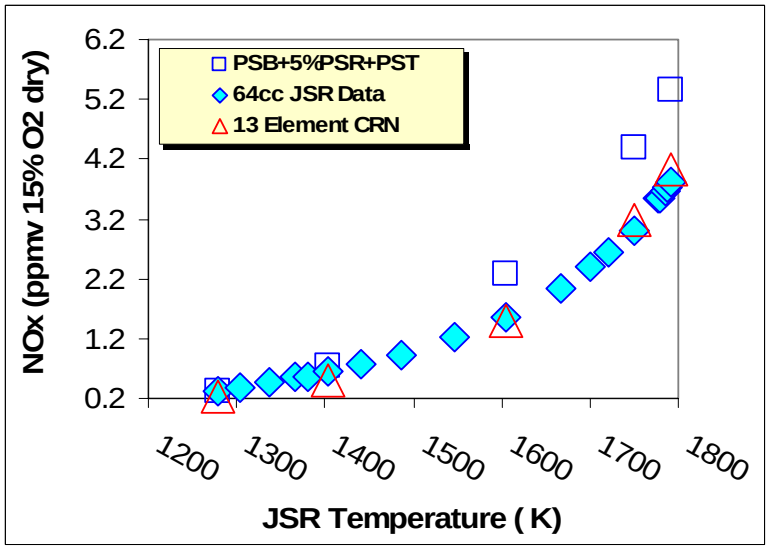

Figure 9: Measured NOx versus measured combustion temperature for 64 cm^3 JSR with 5.6 mm nozzle burning hydrogen. SPP injector outlet temperature = 32-39 C. Predictions of Novosselov [13] using 3-element model (PSB + 5%PSR + PST) 13-element CRN also shown.

3. Hydrogen Flashback Studies

Experiments were carried out to determine the conditions under which the lean hydrogen flame would flash back into the injector. The 64 cm^3 JSR with 6.35 mm tube and spoke injector were used. Two modes were observed: flame burning/anchored in the nozzle (only nozzle temperature increased) and flame burning in the injector (temperature increase throughout the injector). Nozzle burning was a necessary precursor to injector flashback and would initiate at injector velocities around 20-25 m/s. A further, small decrease in velocity (18-20 m/s) would cause the flame to flash back into the injector. As shown in Figure 10, injector flashback occurs at the same fuel-air equivalence ratio (phi) as nozzle burning, but at lower velocities. Both injector flashback and nozzle burning show a strong hysteresis. Velocities of approximately 45 m/s are required to push the flame back out of the injector and velocities of nearly 90 m/s are required to move the flame back off the nozzle.

Similar experiments with pure CH_4 and C_2H_4 could not initiate nozzle burning even at velocities as low as 15 m/s.

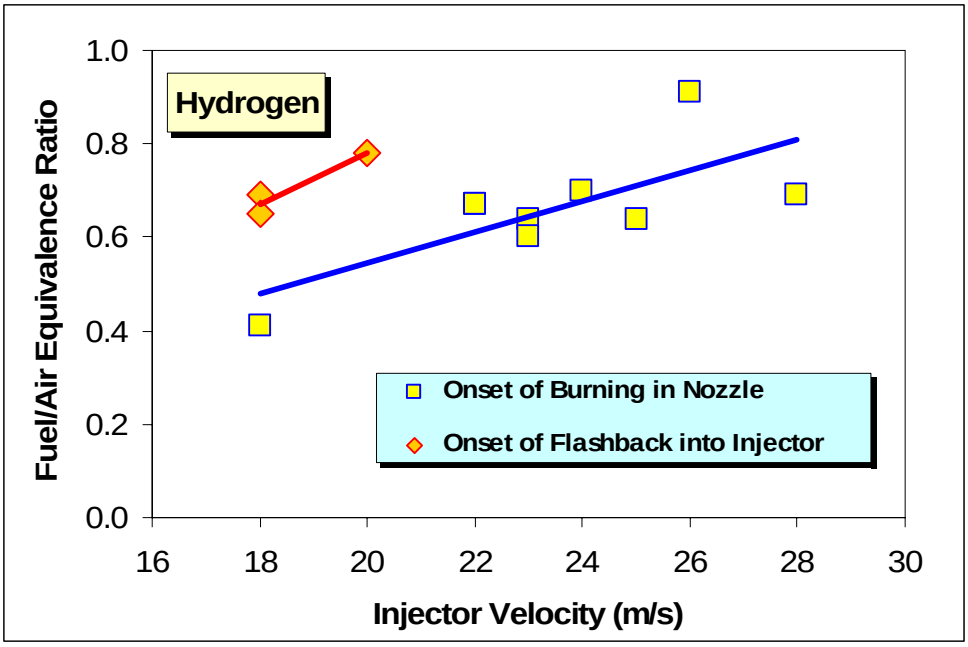

Figure 10: Measurements of hydrogen flashback tendencies due to Polagye [14]. Using 64 cm^3 JSR with 6.35 mm tube and spoke injector of Figure 4. Onset of two situations plotted: 1) burning in nozzle without propagation of flame upstream into injector, 2) flashback into injector. No air and fuel preheat used. Injector velocity based on air and hydrogen flow rates at unheated inlet condition (room temperature).

4. Modeling

Novosselov [13] has modeled the 64 cm^3 JSR using the chemical reactor network (CRN) approach. Predictions of NOx and CO by the CRN approach are compared to measurements. This includes:

- NOx measurements for H_2 combustion, Figure 9 above.
- NOx measurements for selected hydrocarbon fuels of Figure 7, compared in Figure 12 below.
- CO measurements for selected hydrocarbon fuels of Figure 7, compared in Figure 13 below.

Modeled NO is taken equivalent to measured NOx.

The University of Washington chemical reactor code with the detailed chemical kinetic mechanism GRI 3.0 is used for the hydrocarbon fuels modeling. Two arrangements of chemical reactor elements are examined: 3-element scheme and 13-element CRN. The 3-element model consists of three perfectly stirred reactors (PSRs) in series. The methodology of using this reactor arrangement can be found in J.C.Y. Lee, Malte, and Benjamin [9]. The first reactor in the series is a PSB (PSR at incipient blowout). The second reactor is an adiabatic PSR with 5% of the total JSR volume. The third reactor is a PST (PSR at the assigned temperature). The assigned temperature is the measured temperature corrected for the thermocouple heat loss. The volume of the PSR 3 is the remaining 93-94% of the JSR cavity.

The PSB exhibits high concentration of free radicals and occupies a very small volume of the JSR – from 1.3 to 2.3% (the largest volume corresponds to methane and the smallest to ethylene combustion). The reactor represents the flame front in the JSR. The NO formation rate is relatively small due to the low (blowout) temperature in this element. The second element is 5% of the total JSR volume. It represents the main flame, with free radicals at super-equilibrium concentration. PSR 2 has high NO production rate due to its high temperature and free radical concentrations. The third element represents the post-flame recirculation zone of the JSR. With most of the species in this zone relaxing towards equilibrium concentration, the NO formation rate is relatively low. The temperature in the element is not high enough (1790K) to trigger significant amounts of thermal NO.

The 13-element model is a more elegant representation of the combustion process in the JSR. In order to represent the flame that surrounds the incoming jet, the domain is divided into three streams, each of which has a PSB followed by a PSR. These are illustrated in the CRN diagram of Figure 11. Reactors 7 and 8 are on jet centerline, while reactors 3 and 4 are on the outer edge of the jet. The two reactors of each stream are assumed adiabatic. Each stream receives fresh fuel-air mixture in the first element (PSB) and the recirculation zone gas entrained by the jet action in the second element (PSR). The ignition of the fresh fuel air mixture occurs in the PSB elements 3, 6 and 7. After entraining some of the gas from the recirculation zone the combustion continues in the PSR elements 4, 5 and 8 at super-equilibrium levels of free radicals and at high

temperature. The recirculation zone of the JSR is represented by a PSR element assigned the measured combustion temperature (this is element 9). The exhaust flow of the reactor is modeled as a PFR element.

Although CFD simulations have not been performed for the JSR geometry, flow splits between the elements in the 13-element CRN are chosen by Novosselov [13] partly based on CFD results for the primary zone of a can-type gas turbine combustor and the literature. The CRN flow splits are tuned to obtain the best agreement with the experimental data for the methane-fired JSR (Figure 7). Figure 11 shows the 13-element CRN with the flow splits between the elements. The outer jet stream (PSB 3-PSR 4) receives 50% of the total jet fuel-air mixture due to larger area associated with the greater radius. The rest of the flow is divided in half between the two other streams PSB 6-PSR 5 and PSB 7-PSR 8, which are located closer to the center of the jet. The second element in each series treats the combustion of the mixture of ignited fresh mixture from the PSB element and entrained recirculating gas.

The total jet entrainment defines the flow split between element MIX 10 and PFR 13. The flow fraction that is entrained by the jet passes through MIX 10. It is determined based on the jet entrainment relation applied to the jet-stirred reactor by Thornton, Malte, and Crittenden [5] and calculated to be 80% of the jet mass flow. Consequently 20% of the recirculation zone mass flow is exhausted (PFR 13). The probe for gas sample measurement is inserted into the recirculation zone. The flow conditions and the species concentrations inside of the probe are similar to those of the exhaust ports. Thus, in this modeling, it is assumed that the sampled gas is the same as the exhaust gas. PFR 13 also represents the interior of the uncooled sample probe tip though which the sampled gas is pulled from the JSR. PFR 13 has a short residence time and thus has little effect on the NOx (typically 0.1-0.2 ppmv).

The recirculation gas is entrained by the jet in two different locations of the CRN. First, a small part (3%) is entrained near the bottom of JSR into PSR 4, the rest of the recirculating gas is entrained by the half length distance of the JSR into PSR 5. PSR 4 is modeled as an adiabatic element, the local temperature in this element is 10-20 K higher then the temperature measured in the recirculation zone. The gas from PSR 4 enters PSR 5 along with the majority of the recirculating gas. The temperature in this element is only slightly higher than in the recirculation zone. Finally, the gas from the PSR 5 mixes with the freshly ignited mixture from PSB 7 and enters PSR 8. The temperatures in the PSR elements are determined by adiabatic combustion diluted with recirculating gas at the measured corrected temperature.

Hydrogen Combustion: Measured NOx for hydrogen combustion, compared to the modeling predictions is shown above in Figure 9. The results are modeled using the modified GRI 3.0 mechanism and the 3-element scheme and the 13-element CRN. The 13-element CRN results show reasonably close agreement to the measurements. As shown on Figure 9, the modeled NOx (adjusted to 15% O_2) is within 0.3 part per million of the measurements for the 13-element CRN. However, the 3-element model is

somewhat off for this case, over predicting the NOx by about 2 ppmv at the highest temperature run.

The kinetic mechanism used is a modified version of GRI 3.0. The modification is conducted by substituting the Konnov and de Ruyck [15] temperature-dependent rate constant for the reaction: NNH + O → NH + NO. In the unmodified GRI 3.0 mechanism, this rate constant has zero activation energy, which causes the reaction rate to remain high at the reduced temperature levels of interest in lean-premixed, low-NOx combustion. This leads to over prediction of the NO formation. The problem is most severe at low pressure for H_2 combustion, because of the high levels of super equilibrium H and O generated, which give rise to increased NO formed from the NNH chemistry.

By making this single change to GRI 3.0, good agreement is obtained between the NO predictions and NOx measurements for both hydrogen atmospheric pressure combustion (this paper) and 6.5 atm combustion of H_2-CO blends (see [13]). The activation energy of NNH + O → NH + NO is taken as 16.8 kJ/mol (4 kcal/mol), which is in the center of the suggested range and the pre-exponential constant is taken as 10^{14} cm^3/mol/s, which is at the minimum of the range recommended by Konnov and de Ruyck [15].

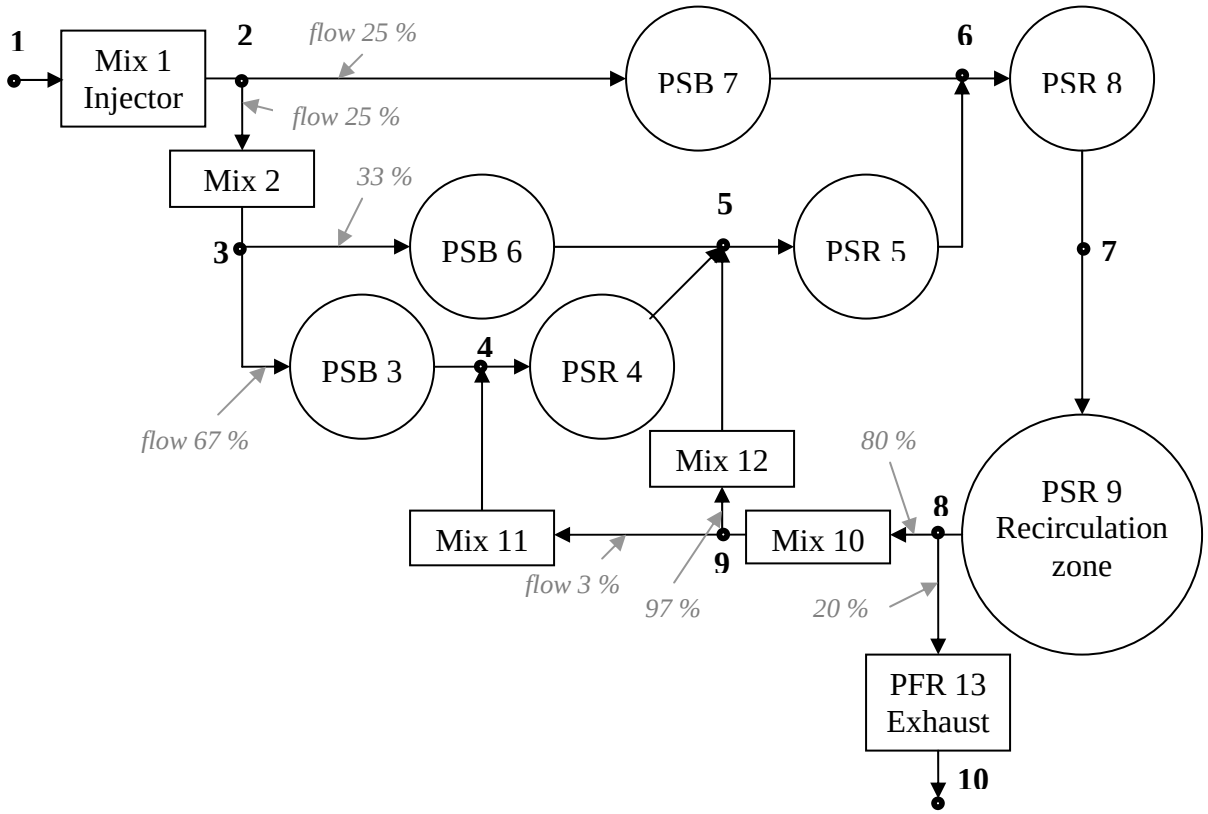

Figure 11: 13-element chemical reactor network (CRN) model for single-jet stirred reactor due to Novosselov [13].

Hydrocarbon Flames: The NO formation routes vary depending on position in the JSR. Since the flame front is modeled as a PSB, the temperature in the these elements is not high enough to form significant amounts of NO via the prompt, N_2O, and Zeldovich mechanisms due to the exponential temperature dependency in the rate expressions. However, the NNH formation route in GRI3.0 mechanism (modified Bozzeli and Dean [16]) does not have temperature dependency in NO formation rate. The NNH mechanism becomes active at the low temperature condition of the PSB element and contributes up to 2 ppmv NO corrected to 15% O_2, which is about 30% of the total NO for the JSR. PSR 4 in the 13-element CRN is the largest NO producer due to its high temperature and high free radical concentrations. Elements PSR 5 and PSR 8 have a large amount of recirculation gas entrained, which reduces the temperature in these elements as well as their free radical counts. The NO formation in elements PSR 5 and PSR 8 is due to the relatively active N_2O pathway; the NNH and prompt pathways contributions are small.

Figure 12 shows the NO_x results of modeling for both the 3-element and 13-element models applied to the hydrocarbon fuel experiments of Figure 7. Generally, both models show very good agreement with the data. The 13-element CRN can be further tuned to obtain better agreement with the data; however, in this study this has not been done due to the lack of detailed flow field information. Figure 13 shows the CO results, which are in reasonably good agreement with the experimental data.

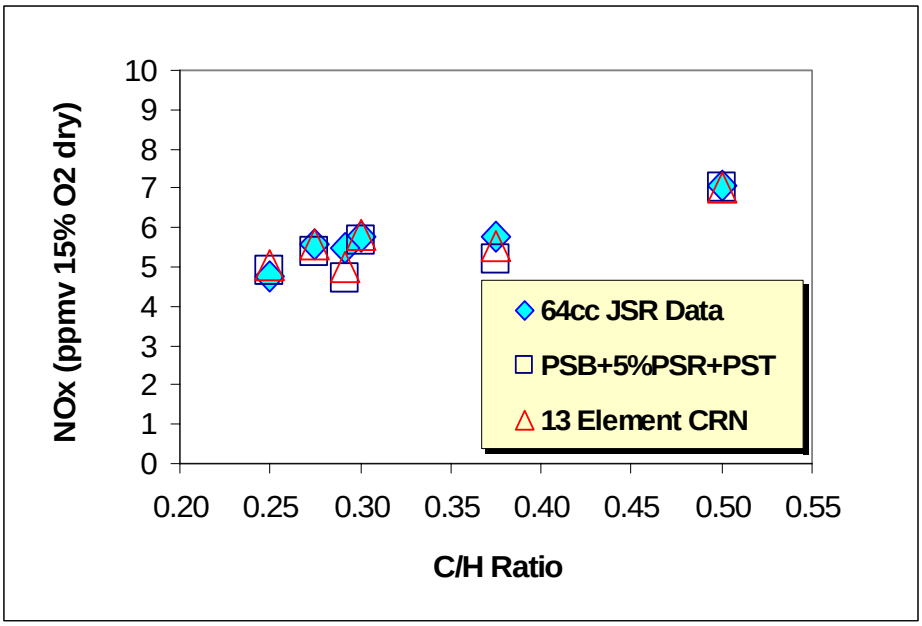

Figure 12: Comparison of NOx data from Figure 6 with predictions by the 3-element and 13-element models of Novosselov [13].

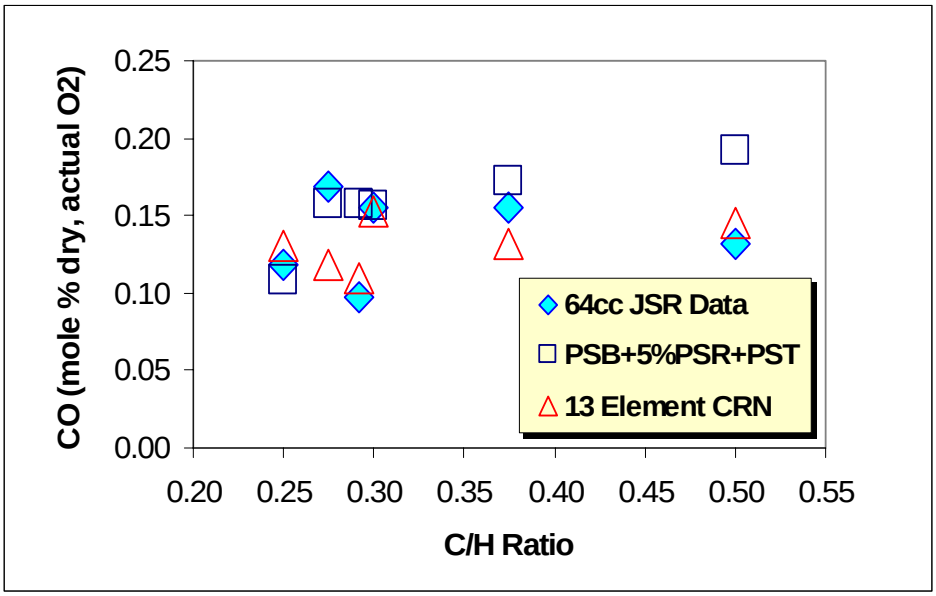

Figure 13: Comparison of CO data (corresponding to the NOx data of Figure 6) with predictions by the 3-element and 13-element models of Novosselov [13].

References

[1] Longwell, J.P., Weiss, M.A., *Industrial and Engineering Chemistry* 47 (1955) 1634-1643.

[2] Pratt, D.T., Starkman, E.S., *Proceedings of the Combustion Institute* 12 (1968) 891-899.

[3] Jenkins, D.R., Yumlu, V.S., Spalding, D.B., *Proceedings of the Combustion Institute* 11 (1966) 779-790.

[4] Malte, P.C., Pratt, D.T, *Combustion Science and Technology* 9 (1974) 221-231.

[5] Thornton, M.M., Malte, P.C., Crittenden, A.L., *Combustion Science and Technology* 54 (1987) 275-297.

[6] Steele, R.C, Malte, P.C., Nicol, D.G., Kramlich, J.C., *Combustion and Flame* 100 (1995) 440-449.

[7] Steele, R.C., Tonouchi, J.H., Nicol, D.G., Horning, D.C., Malte, P.C., Pratt, D.T., *Journal of Engineering for Gas Turbines and Power* 120 (1998) 303-310.

[8] Rutar, T., Malte, P.C., Kramlich, J.C., *Proceedings of the Combustion Institute* 28 (2000) 2435-2441.

[9] Lee, J.C.Y., Malte, P.C., Benjamin, M.A., *Journal of Engineering for Gas Turbines and Power* 125 (2003) 861-871.

[10] Edmonds, R., "Prevaporized and premixed combustion at short residence times," Master of Science Thesis, Dept. of Mech. Engr., Univ. of Washington, Seattle, WA (2002). (This may be accessed online at the address *www.energy.washington.edu*, denoting "laboratory," followed by "publications.")

[11] Lee, A.C., "Experimental investigation of liquid fuel vaporization and mixing in steam and air," Master of Science Thesis, Dept. of Mech. Engr., Univ. of Washington, Seattle, WA (2003). (This may be accessed online at the address *www.energy.washington.edu*, denoting "laboratory," followed by "publications.")

[12] Fackler, K.B., "Gaseous fuel interchangeability," graduate research, Dept. of Mech. Engr., Univ. of Washington, Seattle, WA (2006).

[13] Novosselov, I.V., "Chemical reactor networks for combustion systems modeling," PhD Dissertation, Dept. of Mech. Engr., Univ. of Washington, Seattle, WA (2006). (This may be accessed online at the address *www.energy.washington.edu*, denoting "laboratory," followed by "publications.")

[14] Polagye, B.L., "Hydrogen combustion," graduate research, Dept. of Mech. Engr., Univ. of Washington, Seattle, WA (2005).

[15] Konnov, A.A.; De Ruyck J., *Combustion and Flame* 125 (2001) 1258-1264.

[16] Bozzelli, J.W.; Dean, A.M., *International Journal of Chemical Kinetics* 27 (1995) 1097-1105.

APPENDIX

Table A1: SPP and JSR data for methane and light naphtha burned in 16 cm^3 JSR; due to Edmonds [10].

	16 cc JSR									
FUEL	**Methane**					**Light Naphtha**				
Chemical Formula	CH_4	CH_4	CH_4	CH_4	CH_4	$C_{5.9}H_{12.5}$	$C_{5.9}H_{12.5}$	$C_{5.9}H_{12.5}$	$C_{5.9}H_{12.5}$	$C_{5.9}H_{12.5}$
S ppm wt	0	0	0	0	0	9	9	9	9	9
N ppm wt	0	0	0	0	0	<1	<1	<1	<1	<1
SPP										
Atom air (slpm)	5	5	5	5	5	5	5	5	5	5
Stage 1 air (slpm)	30	30	30	30	30	30	30	30	30	30
Stage 2 air (slpm)	100	100	100	100	100	100	100	100	100	100
Total air (slpm)	135	135	135	135	135	135	135	135	135	135
Stage 1 T (deg C)	150	250	300	390	405	150	250	300	370	390
Stage 2 T (deg C)	250	355	400	500	550	250	350	400	500	550
Stage 1 time (ms)	13.8	11.6	10.7	9.7	9.6	15.0	12.5	11.4	10.3	10.1
Stage 2 time (ms)	8.8	7.4	7.0	6.3	6.0	9.1	8.0	7.2	6.4	6.1
Total res time (ms)	22.6	19.0	17.7	16.0	15.6	24.1	20.5	18.6	16.7	16.2
Stage 2 P (psig)	11.8	12.0	12.5	13.3	13.5	11.5	12.8	12.0	12.5	12.0
JSR										
Volume (cm^3)	15.8	15.8	15.8	15.8	15.8	15.8	15.8	15.8	15.8	15.8
Diameter jet (mm)	4.0	4.0	4.0	4.0	4.0	4.0	4.0	4.0	4.0	4.0
Velocity jet (m/s)	242	289	309	353	375	231	275	296	340	362
Res time (ms)	1.5	1.5	1.5	1.5	1.5	1.5	1.5	1.4	1.4	1.4
Phi by gas analysis	0.65	0.59	0.57	0.51	0.49	0.61	0.57	0.54	0.50	0.47
T measured (deg C)	1490	1480	1480	1478	1478	1475	1475	1480	1477	1478
T corrected (K)	1793	1783	1783	1781	1781	1778	1778	1783	1780	1781
CO2 (mole% dry)	6.9	6.3	6.0	5.5	5.2	8.3	7.7	7.4	6.7	6.4
O2 (mole % dry)	7.7	8.9	9.2	10.7	11.2	8.3	9.2	9.9	10.8	11.3
CO (mole% dry)	0.24	0.22	0.21	0.17	0.15	0.28	0.25	0.26	0.23	0.21
NOx (ppm vol dry)	8.9	7.1	6.8	5.8	5.7	10.8	10.0	9.2	8.2	8.0
NOx (ppmv 15% O2 dry)	4.0	3.5	3.4	3.4	3.5	5.1	5.1	4.9	4.8	4.9

Table A2: SPP and JSR data for light naphtha and low-sulfur #2 diesel burned in 16 cm^3 JSR; due to Edmonds [10].

	16 cc JSR								
FUEL	**Light Naphtha**					**#2 Diesel**			
Chemical Formula	$C_{5.9}H_{12.5}$	$C_{5.9}H_{12.5}$	$C_{5.9}H_{12.5}$	$C_{5.9}H_{12.5}$	$C_{5.9}H_{12.5}$	$C_{13.8}H_{26.3}$	$C_{13.8}H_{26.3}$	$C_{13.8}H_{26.3}$	$C_{13.8}H_{26.3}$
S ppm wt	9	9	9	9	9	195	195	195	195
N ppm wt	<1	<1	<1	<1	<1	124	124	124	124
SPP									
Atom air (slpm)	5	5	5	5	5	5	5	5	5
Stage 1 air (slpm)	50	50	50	50	50	30	30	30	30
Stage 2 air (slpm)	100	100	100	100	100	100	100	100	100
Total air (slpm)	155	155	155	155	155	135	135	135	135
Stage 1 T (deg C)	150	250	300	388	420	250	300	365	389
Stage 2 T (deg C)	250	350	400	500	550	350	400	500	550
Stage 1 time (ms)	10.4	8.6	7.9	7.1	6.8	12.7	11.8	10.6	10.4
Stage 2 time (ms)	8.6	7.4	6.9	6.2	5.8	7.9	7.4	6.4	6.2
Total res time (ms)	19.0	16.0	14.8	13.3	12.6	20.6	19.2	17.0	16.6
Stage 2 P (psig)	13.8	14.3	14.5	15.5	15.5	12.3	12.5	12.5	13.0
JSR									
Volume (cm^3)	15.8	15.8	15.8	15.8	15.8	15.8	15.8	15.8	15.8
Diameter jet (mm)	4.0	4.0	4.0	4.0	4.0	4.0	4.0	4.0	4.0
Velocity jet (m/s)	265	315	340	390	416	273	295	338	360
Res time (ms)	1.3	1.3	1.3	1.3	1.3	1.4	1.4	1.4	1.4
Phi by gas analysis	0.60	0.56	0.54	0.50	0.47	0.57	0.54	0.51	0.50
T measured (deg C)	1480	1480	1480	1480	1478	1477	1480	1478	1480
T corrected (K)	1783	1783	1783	1783	1781	1780	1783	1781	1783
CO2 (mole% dry)	8.2	7.6	7.3	6.8	6.4	8.0	7.7	7.2	7.0
O2 (mole % dry)	8.6	9.5	10.0	10.8	11.3	9.3	9.8	10.5	10.7
CO (mole% dry)	0.29	0.25	0.24	0.19	0.18	0.27	0.24	0.24	0.23
NOx (ppm vol dry)	10.4	9.4	9.0	8.6	8.1	12.9	12.9	11.1	11.6
NOx (ppmv 15% O2 dry)	5.0	4.9	4.9	5.0	5.0	6.6	6.9	6.3	6.8

Table A3: SPP and JSR data for various fuels burned in 16 and 64 cm^3 JSRs; due to Edmonds [10], A.C. Lee [11], and Fackler [12].

	16 cc JSR				64 cc JSR				
FUEL	#2 Diesel				80% Meth/20% Prop	Propane	#2 Diesel		
	Edmonds				Fackler	A.C. Lee	A.C. Lee		
Chemical Formula	$C_{13.8}H_{26.3}$	$C_{13.8}H_{26.3}$	$C_{13.8}H_{26.3}$	$C_{13.8}H_{26.3}$	$C_{1.39}H_{4.79}$	C_3H_8	$C_{13.8}H_{26.3}$	$C_{13.8}H_{26.3}$	$C_{13.8}H_{26.3}$
S ppm wt	195	195	195	195	0	0	195	195	195
N ppm wt	124	124	124	124	0	0	124	124	124
SPP									
Atom air (slpm)	5	5	5	5	0	5	5	5	5
Stage 1 air (slpm)	50	50	50	50	75.5	50	50	90	100
Stage 2 air (slpm)	100	100	100	100	72	100	100	100	100
Total air (slpm)	155	155	155	155	147.5	155	155	195	205
Stage 1 T (deg C)	250	300	400	436	219	400	401	352	336
Stage 2 T (deg C)	350	400	500	550	219	522	523	500	499
Stage 1 time (ms)	8.9	8.2	7.1	6.8	4.0	4.8	4.5	3.1	2.9
Stage 2 time (ms)	7.5	7.0	6.3	5.9	5.2	3.7	3.7	3.3	3.2
Total res time (ms)	16.4	15.2	13.4	12.7	9.2	8.5	8.2	6.4	6.1
Stage 2 P (psig)	14.8	15.0	15.8	15.9	0.5	4.0	4.0	5.8	6.0
JSR									
Volume (cm^3)	15.8	15.8	15.8	15.8	64.0	64.0	64.0	64.0	64.0
Diameter jet (mm)	4.0	4.0	4.0	4.0	9.0	5.6	5.6	5.6	5.6
Velocity jet (m/s)	313	338	388	413	67	282	268	328	344
Res time (ms)	1.3	1.3	1.3	1.3	4.5	4.3	4.2	3.4	3.2
Phi by gas analysis	0.55	0.53	0.51	0.49	0.57	0.54	0.53	0.53	0.53
T measured (deg C)	1476	1476	1480	1480	1489	1483	1482	1485	1482
T corrected (K)	1779	1779	1783	1783	1792	1786	1785	1788	1785
CO2 (mole% dry)	7.8	7.5	7.2	6.9	6.7	6.9	7.6	7.5	7.4
O2 (mole % dry)	9.6	10.0	10.4	10.8	9.8	9.8	9.9	9.9	10.0
CO (mole% dry)	0.22	0.21	0.23	0.22	0.13	0.10	0.13	0.14	0.14
NOx (ppm vol dry)	12.4	11.7	11.1	11.1	8.2	11.0	14.5	14.0	13.3
NOx (ppmv 15% O2 dry)	6.5	6.4	6.3	6.5	4.3	5.8	7.8	7.5	7.2

Table A4: 64 cm^3 JSR with 5.6 mm nozzle burning methane, ethylene, and C_1-C_4 alkane blends.

C/H Ratio	T-comb (K)	T-premix (deg C)	tau (ms)	phi	NOx (ppmv 15%O2 dry)
0.250	1792	300	3.72	0.643	4.87
0.250	1795	300	3.69	0.655	5.14
0.250	1792	300	3.66	0.653	4.79
0.250	1790	300	3.71	0.657	4.93
0.250	1792	210	3.61	0.673	4.43
0.250	1791	210	3.62	0.669	4.46
0.250	1792	300	3.64	0.632	4.61
0.250	1791	300	3.63	0.635	4.53
0.250	1792	150	3.69	0.695	4.65
0.250	1791	150	3.68	0.693	4.64
0.250	1791	210	3.65	0.670	4.32
0.250	1791	300	3.68	0.642	4.80
0.250	1790	300	3.67	0.647	4.71
0.250	1791	250	3.61	0.665	4.62
0.250	1791	300	3.64	0.668	4.72
0.274	1789	300	3.66	0.628	4.59
0.283	1791	210	3.64	0.668	4.84
0.292	1795	300	3.69	0.642	5.56
0.300	1795	300	3.67	0.630	5.65
0.301	1795	300	3.73	0.631	5.79
0.308	1795	300	3.69	0.635	5.97
0.308	1791	210	3.63	0.659	5.11
0.308	1794	300	3.61	0.624	5.23
0.308	1792	300	3.66	0.629	5.26
0.308	1792	300	3.66	0.624	5.34
0.330	1790	300	3.62	0.623	5.45
0.332	1792	210	3.63	0.659	5.29
0.335	1791	210	3.63	0.657	5.31
0.343	1791	210	3.63	0.655	5.29
0.346	1794	300	3.62	0.623	5.51
0.353	1790	300	3.62	0.620	5.80
0.375	1790	300	3.71	0.230	5.85
0.500	1795	300	3.76	0.577	7.55
0.500	1794	300	3.75	0.580	6.52
0.500	1790	300	3.78	0.575	7.30
0.500	1791	300	3.73	0.560	6.78

Table A5: 64 cm^3 JSR with 5.6 mm nozzle burning $H_2/CO/CO_2$ blends.
C/H ratio is based on CO/H_2 ratio. CO_2 is 20 mole %.

C/H Ratio	T-comb (K)	T-premix (deg C)	tau (ms)	phi	NOx (ppmv 15% O2 dry)
0.167	1791	150	3.57	0.647	2.93
0.167	1791	210	3.56	0.618	3.16
0.167	1791	225	3.58	0.611	3.12
0.167	1790	250	3.58	0.601	3.11
0.501	1791	150	3.59	0.595	3.28
0.500	1791	200	3.61	0.571	3.73
0.500	1792	250	3.62	0.558	3.91
1.503	1790	150	3.59	0.612	4.58
1.500	1791	200	3.62	0.597	5.21
1.500	1790	250	3.60	0.569	5.48

Table A6: 64 cm^3 JSR with 5.6 mm nozzle burning hydrogen.

T-comb (K)	T-premix (deg C)	nozzle vel (m/s)	tau (ms)	phi	O2 (mole % dry)	NOx (ppmv 15% O2 dry)
1279	32	121	5.51	0.380	14.58	0.31
1304	32	121	5.39	0.395	14.28	0.39
1336	32	122	5.23	0.415	13.87	0.47
1367	33	124	5.09	0.435	13.57	0.56
1381	33	124	5.04	0.439	13.47	0.57
1404	34	124	4.96	0.443	13.28	0.65
1441	34	125	4.81	0.466	12.78	0.76
1486	34	126	4.64	0.492	12.29	0.93
1546	34	127	4.44	0.518	11.59	1.21
1605	35	129	4.26	0.551	10.89	1.56
1667	36	131	4.08	0.578	10.19	2.02
1700	36	131	4.02	0.598	9.80	2.38
1722	37	132	3.95	0.609	9.50	2.63
1751	37	133	3.87	0.626	9.11	3.00
1778	38	133	3.81	0.641	8.81	3.52
1780	38	133	3.81	0.641	8.72	3.54
1785	38	134	3.79	0.645	8.73	3.64
1788	38	134	3.79	0.645	8.64	3.71
1791	39	134	3.78	0.650	8.65	3.80